FEKO/NEC2 Simulation of Candidate Antennas for the Long Wavelength Array (LWA)

Nassissie Fekadu [1, 2] and Amir I. Zaghloul [1, 3]

[1] Virginia Polytechnic Institute and State University
Blacksburg, VA 24061-2000, USA
nfekadu@vt.edu , amirz@vt.edu

[2] Noblis
3150 Fairview Park Drive
Falls Church, VA 22042-4504, USA
nassissie.fekadu@noblis.org

[3] US Army Research Laboratory
Adelphia, MD 20783, USA
amir.zaghloul@us.army.mil

Abstract **─** This paper presents FEKO and NEC-2 simulations done on three dipole-like structures; the big blade, the tied-fork and the fork antenna. These antenna elements are considered for the design of the long wavelength array (LWA). The LWA is an interferometer under construction in New Mexico, USA for astronomical observations in the 20 - 80 MHz spectrum. This paper presents the simulation results of a co-polarized antenna gain patterns, impedance values, and mutual couplings for each candidate elements. Coupling results from FEKO and NEC-2 simulations are compared with measurement result of the big blade antenna. The paper also presents S-parameters for 25 elements of the tied-fork antennas.

Index Terms**─** Blade, dipole-like structures, FEKO, fork, mutual coupling, and tied-fork.

I. INTRODUCTION

The long wavelength array (LWA) is a radio interferometer telescope array under construction in New Mexico, USA for astronomical observation in the 20-80 MHz radio spectrum, within a total range of 10 MHz (ionospheric cut off) to 88 MHz [1, 2]. The array will consist of 53 electrically steered phased array stations. Each station will be constructed using 256 cross-dipole type antennas. The array will cover maximum baselines (distances between stations) up to 400 km of which core stations of 17 are within the center 10 km [3]. The station array has a pseudo-random arrangement that enables large aperture achievement with relatively fewer antenna elements while maintaining low sidelobe levels [4]. The objective of the LWA is to achieve long wavelength imaging with angular resolution and sensitivity comparable to existing instruments operating at shorter wavelengths [5].

Each station will have an elliptical shape with an axial ratio of 1.1:1 (110m in the N-S direction and 100m in E-W direction). This structure enables observation toward declinations that appear in the southern sky of New Mexico. Furthermore, it provides the ability to observe the inner galaxy region. The dimensions of the station array are chosen to balance sampling of a large field efficiently and calibration across the field of view (FOV) [5]. The array spacing d, is 5m which is 0.33λ at 20MHz and 1.33λ at 80MHz. Aliasing at the highest frequency for periodic arrays is avoided by using spacing, $d < 0.5\lambda$. To avoid aliasing at 80 MHz, the number of antenna elements required for the LWA would have to increase by a factor of three which is economically

Submitted On: July 22, 2010
Accepted On: March 17, 2011

prohibitive [5]. Hence, a pseudo-random array arrangement is used to avoid aliasing at the highest frequency.

The number of elements in a station is arbitrarily chosen to be 256, a power of 2. The number of elements can be anywhere between 50 to 2500; however, it is constrained by requirements such as the baseline which affects image quality and the logistics associated with acquiring land, transporting the data, and maintenance of the equipment [5].

The choice of individual element design depends on whether the design meets technical requirements as well as cost limitations. The technical requirements for the LWA interferometer include [5]:

- Sensitivity on the order of arcseconds resolution of 8" and 2" at 20MHz and 80 MHz, respectively
- Field of view of 8° and 2 ° at 20 MHz and 80 MHz, respectively
- Broad and slowly-varying patterns over the tuning range
- Dimensions on the order of ½ λ at the highest frequency for alias-free beamforming
- Large tuning range for large impedance bandwidth

The technical requirements for candidate elements include [6]:

- Frequency range of 20-80 MHz (3-88 MHz desired)
- Stable, sky noise dominance of 6dB over the frequency range
- Zenith angle coverage, $z \leq 74°$ ($z \leq 80°$ is desired), to detect bright transients near the galactic center
- Good axial ratio for circular polarization (This requirement refers to the cross-polarization isolation)
- Durability for 15 year lifespan

The candidate antennas for the LWA system are dipole-like structures. Even though dipoles inherently have narrow impedances, the limitation does not apply to frequencies below 300MHz. Potential and dominant noise contribution comes from natural Galactic noise, not the instrument used [5].

This paper presents FEKO and NEC-2 simulations of the candidate antennas; the big blade, the tied-fork, and the fork antennas. FEKO is an electromagnetic (EM) analysis software suite based on the method of moments (MoM). NEC-2 (the numerical electromagnetic code version 2) is a public domain code also based on the method of moments. Simulation results from this paper as well as measurement data from other studies show the candidate antennas to be comparable in performance. All three candidates have also shown to meet technical requirements for the element design [2].

Section 2 describes the topology of the three candidate dipole type antennas. Sections 3 and 4 present design specification and design process of the LWA, respectively. Section 5 presents the parameters used for simulating the individual antennas as well as the results of the simulation, including the results from the S-parameter simulation of the 25-element array of tied-fork antennas. Section 6 provides the analysis of the results, and Section 7 summarizes the paper.

II. DESCRIPTION OF CANDIDATE ANTENNAS

Each stand of the candidate antennas has two dipoles with collocated feed points oriented at right angles to each other.

The big blade is a complex structure made of two linearly polarized cross dipoles. The element is made of aluminum sheets. Even though the overall performance of this antenna is comparable with the other candidates, since it takes a total of 13,000 elements to construct the entire array system, it makes this candidate unfavorable with respect to cost. The big blade antenna dimensions are shown in Figure 1 and its images from FEKO and NEC-2 simulations are given in Figure 2.

The tied -fork antenna is made of strands of wire that represent the skeletal outline of the big blade. It also has two bars that run across the strands. Since the fork antenna does not involve the use of the aluminum sheet, it is less costly than the complex big blade structure. The tied-fork antenna dimensions are presented in Fig. 1 and its images from FEKO and NEC-2 simulations are shown in Fig. 2.

Like the tied-fork, the fork antenna is made of 3 strands of wire that represent the skeletal outline of the big blade. This antenna is a cost effective candidate. It is also less susceptible to wind effects [7]. The fork antenna dimensions are presented in Fig. 1 and its images from FEKO and NEC-2

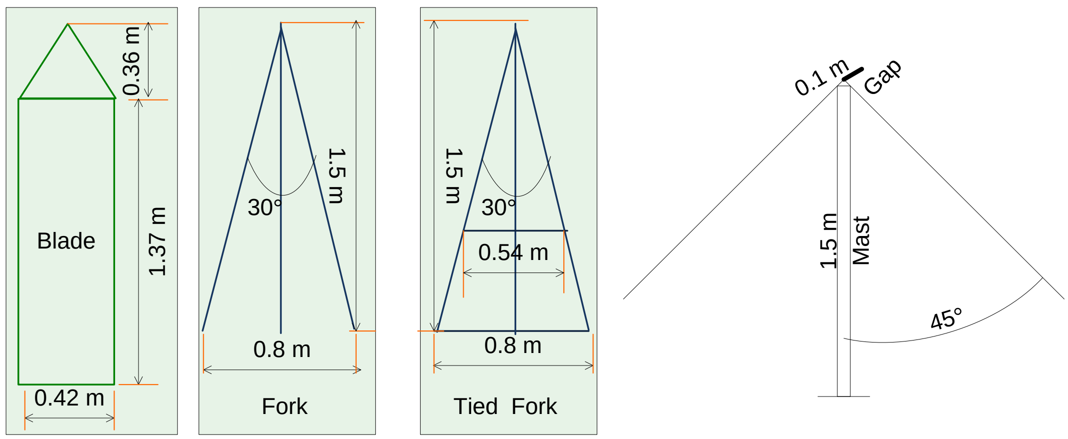

Fig. 1. Big blade, tied fork, and fork antenna dimensions.

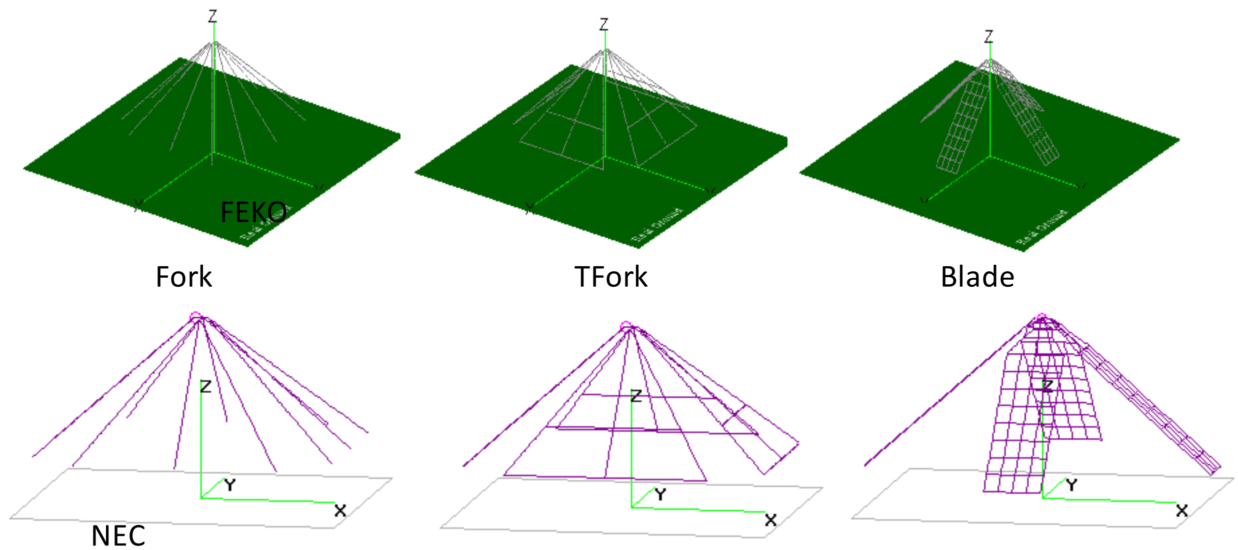

Fig. 2. Big blade, tied fork, and fork images from FEKO and NEC-2 simulations.

simulations are shown in Fig. 2.

III. DESIGN SPECIFICATIONS

The LWA is designed for long-wavelength astrophysics and ionospheric research [5]. The LWA addresses a wide range of research interests including cosmic evolution, solar science, and space weather. Detailed and specific objectives for the LWA are described in [8]. The underlining expectation of the LWA is that it should be able to perform comparably to existing instruments operating in shorter wavelengths with respect to resolution and sensitivity. That is resolution in the order of arcseconds and sensitivity in the orders of mili-janskys, where 1 Jansky= $(10^{-26}\ \mathrm{W})/(\mathrm{m}^2\ \mathrm{Hz}^{-1})$, are desired [5]. This means an improvement of several orders of magnitude over existing instruments operating below 100 MHz [5].

In order to achieve the long wavelength imaging required for the exploration of various scientific frontiers, parameters such as dimensions of stations, resolution, collecting area, sensitivity, and field of view (FOV) are considered in the design process. An overview of these parameters is provided here. However, for detailed description and design processes please refer to [5] and [8]. The key design parameters of the LWA stations are collecting area and dimensions of the station beam [5]. Collecting area contributes to image sensitivity while dimensions of the beam constraint image FOV.

Resolution (R) is the system's ability to distinguish between two very close, adjacent and independent objects in the sky. The largest structure that can be imaged by the system is a function of the observational wavelength and the minimum baseline. It is the finest detail an instrument is capable of showing. It is calculated as, $R= (\lambda/D)*(648000/\pi)$, where D is the maximum baseline (400km).

The process of determining the collecting area involves using sufficient number of sources that are detected above a certain flux within the FOV to calibrate the image against the effects of the ionosphere. The effective collecting area of a LWA station is given by $A= \gamma N_a \, \xi A_{eo} \, (\lambda,\theta,\phi)$ where γ accounts for aggregate mutual coupling, N_a is the number of elements and A_{eo} is the collecting area of a single antenna in isolation [8].

FOV is the area of the sky being observed. Dimensions of the station array determine the width of the station beam which in turn determines the field of view. The image quality over larger FOV is limited by atmospheric variance in it. The usable FOV is determined by spacings between antennas and it is affected significantly by the ionosphere. The FOV of the LWA can be defined as the area bounded by the half-power beamwidth of a station beam and is calculated as $FOV= 4.12\psi_o^2 \, (\lambda/4m)^2 \, (D/100m)^{-2} \sec\theta \, [deg^2]$ where, $\psi_o = 1.02$ for a uniformly excited circular array and D is the station mean diameter. For detail derivation of the parameters, please refer to [8].

The sensitivity of a radiotelescope is a measure of the weakest source of radio emission that can be detected; hence, it is directly related to the errors of measurement [9]. Many factors affect sensitivity including the nature of the source signal, antenna characteristics, receiver performance (LWA has Galactic-noise limited receiver), resolution, the medium between the source and the antenna system (atmospheric conditions that are frequency dependent), image forming characteristics, and the size of the region of the sky observed. Sensitivity is parameterized using system temperature where high system temperature value indicates low sensitivity. Sensitivities are calculated for a given integration time. Sensitivity is proportional to the size of the beam, integration time, and total observation bandwidth. It can be improved after observations by averaging channels together. The sensitivity of observation varies across the FOV where it declines away from the center position of the main beam.

IV. DESIGN PROCESS

In general, for short wavelength design if technical issues are overcome, costs will be a major obstacle [8]. Simulations and prototype testing were performed to choose the design of the antenna elements. Each antenna element needed to achieve large tuning range to be considered for the design of the LWA. Previously, low frequency telescopes used antennas that have inherently large impendence bandwidth such as conical spirals [8]. Since the design of the LWA calls for a large number of antennas, such complex and expensive structures are not suitable for the LWA. Hence, simple wire dipoles (folded dipoles) that have inherently narrow impedance bandwidth are chosen. This does not pose significant problems for systems operating below 300 MHz. This is because the natural Galactic noise dominates over the noise contribution of the electrons attached to the antennas [5]. Prototypes of the antennas are used to measure the radio frequency interference environment in the desired frequency band and the result show stable sky noise dominance of 6dB over the frequency range.

The choice of 256 stands distributed over roughly 100m diameter (110mx100m ellipse) balances the desire to efficiently sample large FOV required to image several sources across the sky against the difficulty of ionospheric calibration across the wide FOV [5]. The LWA will be able to image wide FOVs with sufficient diversity of baselines [8]. This choice will also balance cost against quality of image calibration over a broad range of frequencies and zenith angles [8].

Even though it is desirable to have a small number of stations to simplify the process of obtaining land, transporting data, and maintaining instruments since image quality requires diversity of baselines the argument calls for a larger number of stations. The station numbers (53) were chosen based on prior experience and guidance from previous large array systems [5].

The maximum baseline of 400km was chosen in order to obtain the resolution values required to observe detailed structures of extragalactic radio galaxies and avoid confusion that arises due to unresolved sources or due to plausible long hours of integration times (interval over which data collected are averaged to reduce background noise) [5]. This baseline yields the desired resolution; 8’’ at 20 MHz and 2’’ at 80 MHz.

Optimization of antenna positions for a pseudorandom station configuration was performed and details of it are found in [10]. Pseudorandom antenna distributions are susceptible to mutual coupling effects. Current simulation does not consider effects of coupling for the LWA; future effort will be focused to include effects of coupling. Furthermore, the effects will be studied when the first station is built [8].

As mentioned earlier, the primary receiving element of the LWA is a fixed stand that incorporates two broadband, crossed, linearly-polarized dipoles. The signal from every antenna is processed by a direct-sampling receiver consisting of an analog receiver and an analog-to-digital converter. Beams are formed using a time-domain delay-and-sum architecture, which allows the entire 10–88 MHz passband associated with each antenna to be processed as a single wideband data stream. A finite impulse response filter which is used to introduce coarse delay is also used to introduce corrections for polarization and other frequency-dependent effects. The raw linear polarizations are transformed into calibrated standard orthogonal circular polarizations, and the signals are then added to the signals from other antennas processed similarly [11].

V. SIMULATION PARAMETERS AND RESULTS

This section presents the parameters used and the results obtained from FEKO and NEC-2 simulations. MATLAB scripts are used to generate the antenna models used in the two simulation tools.

Figure 3 shows co-polarized gain patterns in E- and H-planes along with axial ratios of the candidate antennas at 38MHz, 74 MHz, and 80 MHz. The axial ratio resulting from a pair of dipoles can be approximated from the difference between the E- and H-plane gain patterns at each elevation angle for a single dipole [12]. Axial ratios are calculated from the co-polarized gain patterns using $AR(\theta, \phi) = |G_{E,co}(\theta, \phi) - G_{H,co}(\theta, \phi)|$, where (θ, ϕ) are observation angles and GE,co and GH,co are co-polarized gain patterns in the E- and H-planes, respectively, of a single dipole expressed in dB. Since the maximum cross-polarized gains for all antenna structures from both simulation tools are very low, their plots are not included in the paper.

Figure 4 presents impedance values obtained for each isolated dipole-like structure. A reference input impedance of 50 Ω is assumed when calculating the S-parameters in all cases in both FEKO and NEC-2 simulations. Figure 5 shows the S-parameters obtained for two identical elements of each of the antenna types. Dynamic matching at different frequencies would achieve better performance for the significant portion of the required frequency bands instead of the narrow band observed for the S11 values. In Fig. 6, the big blade antenna measurement data from [13] is compared with big blade simulations of NEC-2 and FEKO. A spacing of 6m between two big blade antennas is used when calculating S21.

Figures 7 and 8 present mutual coupling between elements in a periodic 5X5, or 25-element array of tied-fork antennas for the center element and an edge element, respectively, for a range of frequencies. In this coupling calculation all the elements in the array but one are terminated with 50Ω impedance and one of the elements (the edge or the center element) is excited.

A conducting ground screen (3mx3m) that can prevent loss through absorption and isolate the antenna from variable ground conditions to stabilize the system temperature will be used in the field. However, it is not included for this simulation. The measurement setup also did not include the ground screen (Fig. 6). Real ground conditions, permittivity, $\varepsilon_r = 13$, and conductivity, $\sigma = 0.005$ S/m, are used in all cases of the simulation in this study. Based on [14], a wire radius (r_w) = 0.0099 m is used in all cases. A segment length of ~ 8* r_w is used for NEC-2 simulations and a segment length of ~5*r_w is used for FEKO simulations. The choice of the length of the segments is based on [15] and the final adjustments are made by trial and error. The feed point is assumed to be 1.5 m above the ground for all candidate antenna types. A 0.1m feed point width is used for all antenna types.

FEKO and NEC-2 simulation results for the co-polarized E-plane and H-plane gain patterns of the big blade, tied fork, and fork antenna (Fig. 3) at 38 MHz, 74 MHz, and 80 MHz are fairly comparable. The H-plane patterns maintain their shape with increased beamwidth as the frequency increases. However, the E-plane patterns exhibit sidelobes at the higher frequencies. The tied fork antenna has the maximum axial ratio for all frequency ranges. The big blade has the lowest axial ratio in all frequencies at all elevation angles.

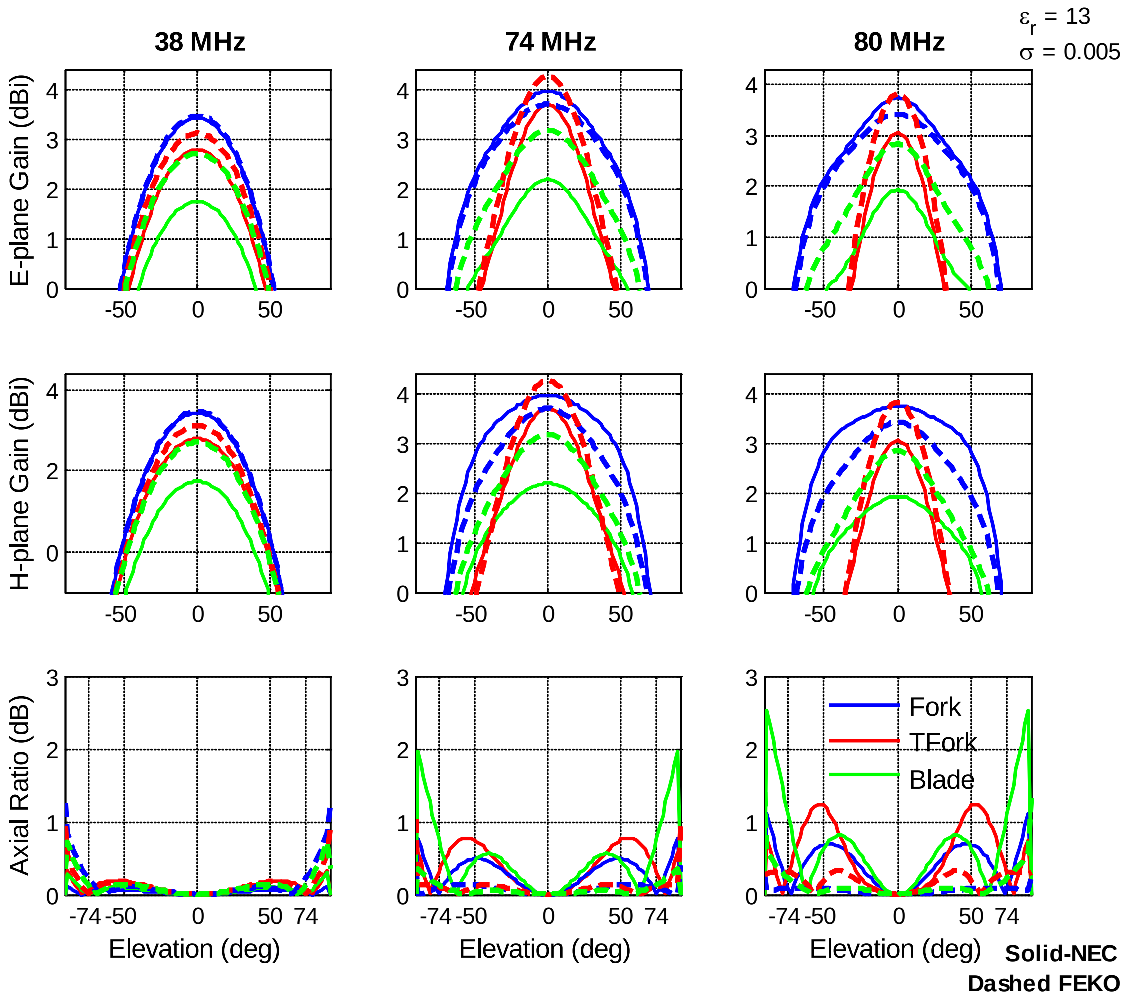

Fig. 3. Co-polarized gain patterns and axial ratios at 38, 74, and 80 MHz.

Impedance values (Fig. 4) obtained from the simulations show that for all the three element types FEKO simulations results are slightly higher, particularly for higher frequencies than NEC-2 simulations. Overall, the fork antenna has higher impedance values than the other two antennas. There is a spike seen around 55 MHz for the fork antenna, and it is assumed to be a simulation artifact. The tied-fork and fork antenna exhibit higher resonant frequencies as compared to the big blade.

For the mutual coupling calculation of two antennas side by side, a spacing of 6 m between the elements is used; this is because the available measurement data is for 6m spacing. However, 5 m spacing is considered for the LWA design. The mutual coupling measurement of the big-blade [13] is comparable with NEC-2 and FEKO simulations results.

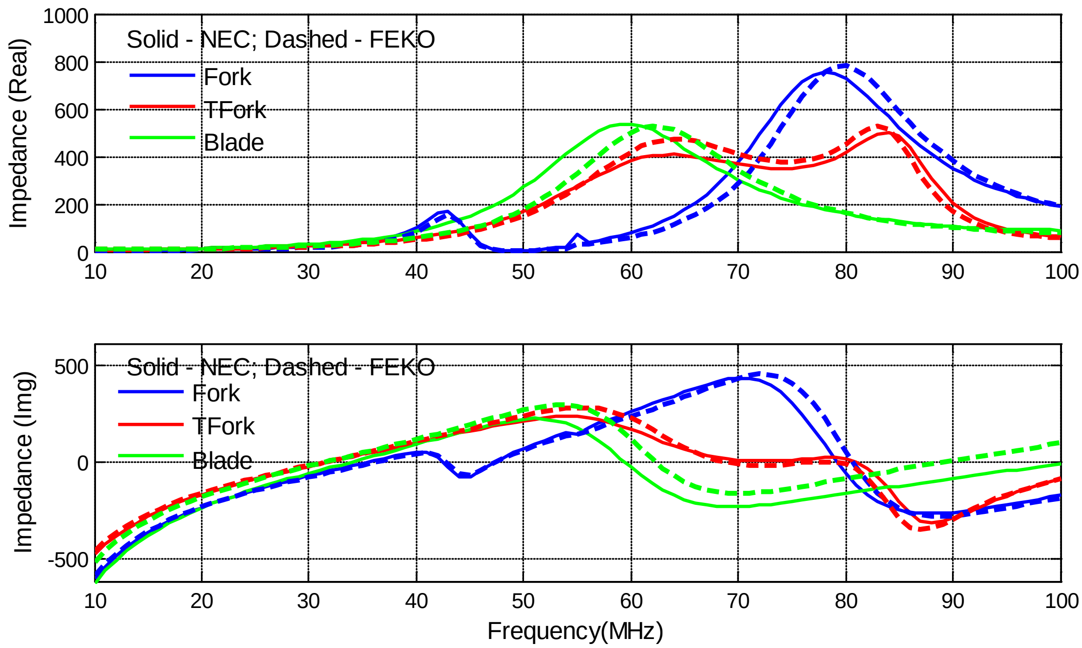

Fig. 4. Big blade, tied-fork, and fork antenna impedances for isolated elements.

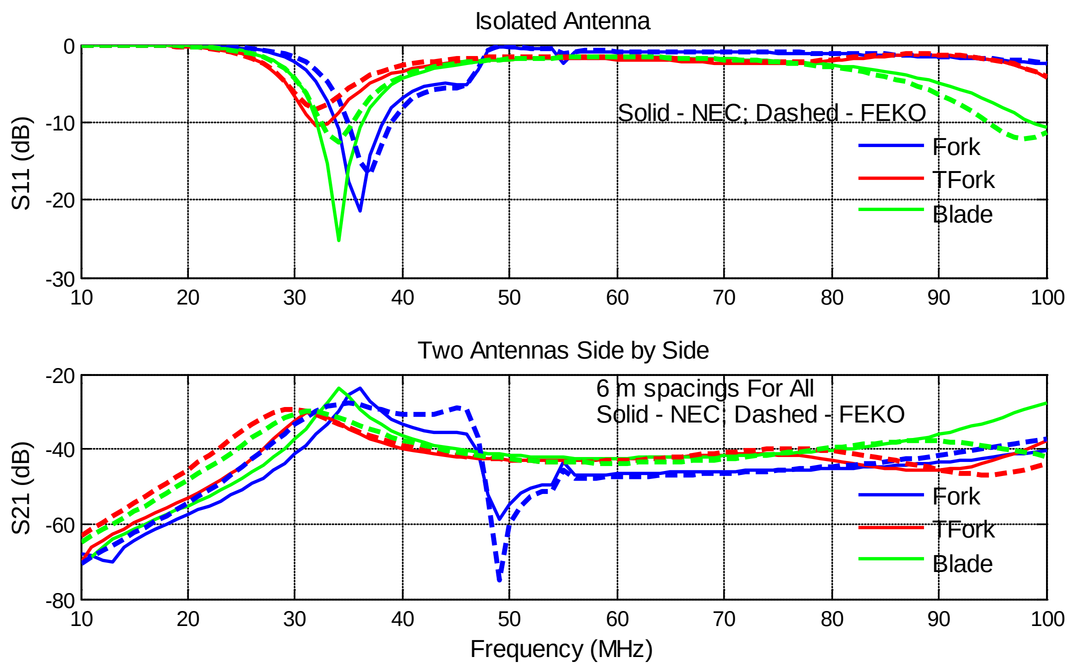

Fig. 5. Big blade, tied-fork, and fork antenna S-parameters.

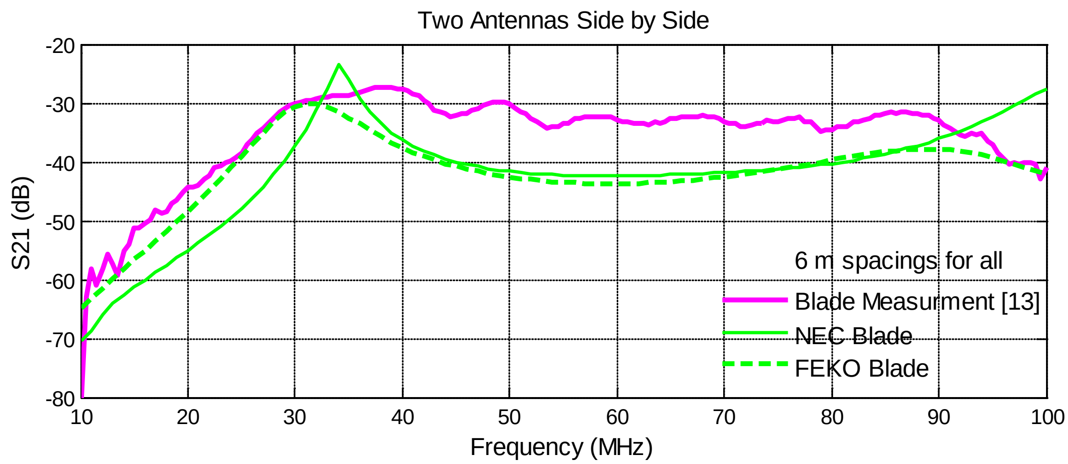

Fig. 6. Measurement data and simulation results of the big blade antenna coupling.

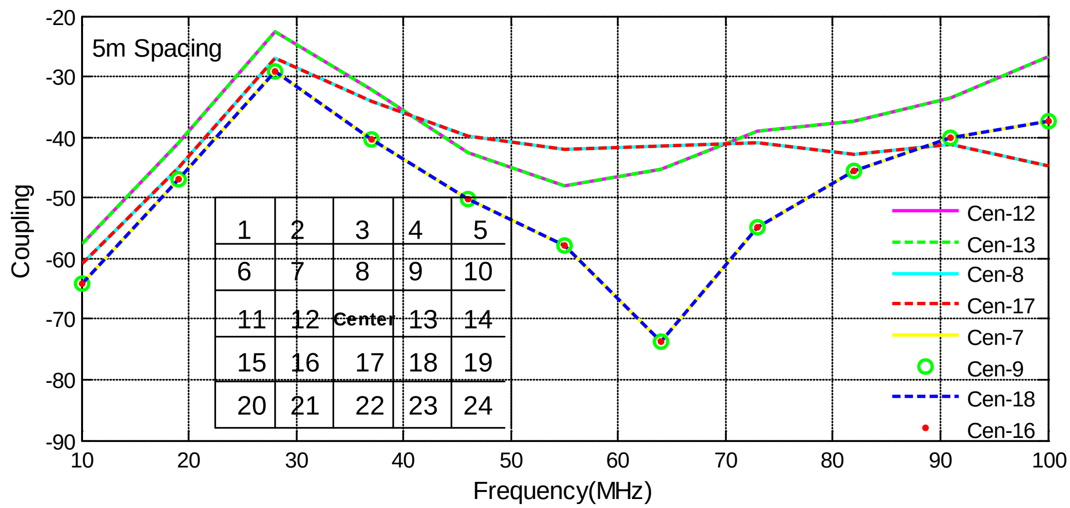

Fig. 7. S-parameters for 5x5 tied-fork antennas – center element.

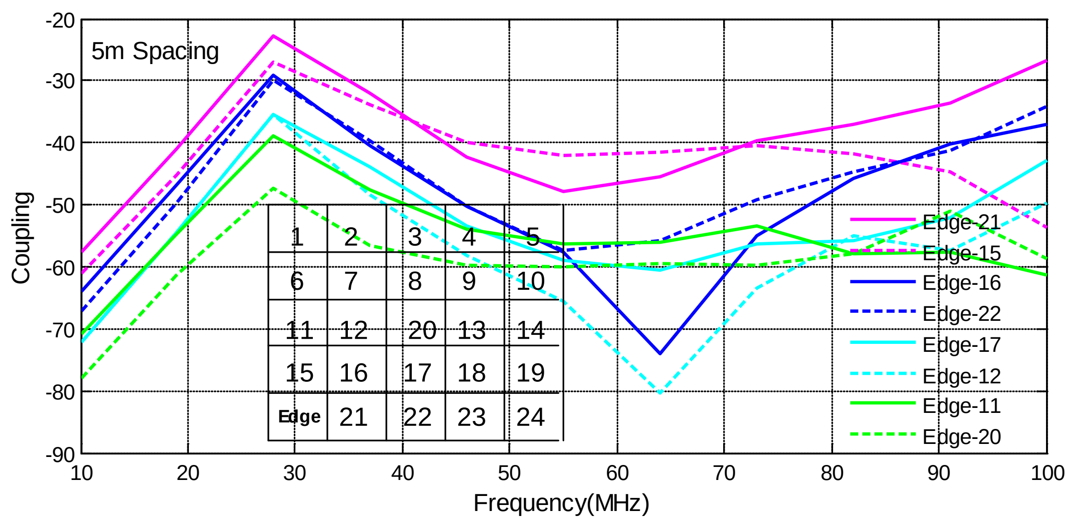

Fig. 8. S-parameters for 5x5 tied-fork antennas – edge element.

VI. ANALYSIS

The LWA candidate antennas maintain good performance over the required 20 – 80 MHz frequency range if a dynamic input impedance matching is applied for frequency and scan angle changes. This study did not consider antenna performance optimization. Even though, the tied-fork antenna and the fork antenna have simpler topology, they exhibit comparable RF properties to the complex big blade structure.

The co-polarized gain patterns of the antennas in both planes exhibit a single, wide beamwidth lobe with the maximum towards zenith. However, the H-plane patterns better maintain their shape and provide increased beamwidth up to higher frequencies than the E-plane patterns, which develop sidelobes at higher frequencies. The fork antenna seems to be better in keeping its shape at all frequencies. The co-polarized gain patterns are plotted only for E-plane since it is assumed the performance of this plane to be worse than other planes [16].

The beam patterns of the three structures have axial symmetry of 1.2 dB or less for elevation angles down to ± 74 ° from zenith for all frequencies. For higher frequencies, the FEKO simulation results show 1dB or less for all frequencies at these elevations.

The simulated impedance values of the simpler topology antennas are generally higher and shifted down in frequency when compared to the simulated response of the big blade antenna. The big blade exhibits larger impedance bandwidth as compared to the other two antennas.

The S-parameters for the 25 tied-fork antennas show that coupling effects are not prominent enough to cause concern. The worst condition, a coupling of -23 dB, is observed for both center and edge cases at 28 MHz at a distance of 5m when the antennas are in parallel. For the same distance if the antennas are placed diagonally from each other, the coupling is only about -27 dB. This is because the induced current is largest when the two antennas are parallel. The coupling results are obtained by exciting one element (center or the edge) and terminating all the other elements with 50 Ω. Note that parallel implies the maximum radiation is aligned along the line of separation, hence a higher coupling. For all the calculation, the unexcited antenna is terminated with a load of 50Ω.

VII. CONCLUSION

FEKO and NEC-2 simulation results of the big blade, tied-fork, and fork antennas are presented in this paper. The candidate antennas exhibit similar characteristics with slight differences in impedance and gain values. The simulation results obtained in this study are in agreement with the measurement provided in [2]. The S-parameters for the 25 tied-fork antennas indicate that coupling is not a concern. However, further analysis is needed to rule it out completely as an important factor affecting pattern.

A dynamic input impedance matching is recommended for the required range of frequencies to obtain optimum performance of the station.

ACKNOWLEDGEMENT

The authors wish to acknowledge the support of Dr. S. Ellingson of Virginia Polytechnic Institute and State University, Dr. N. Kassim, Emil J. Polisensky, Ken Stewart and Henrique Schmitt of the Navy Research Laboratory in providing the measurement data needed for the analysis presented in this paper.

REFERENCES

[1] N. Paravastu, B. Hicks, P. Ray, and W. Erickson, “A New Candidate Active Antenna Design for the Long Wavelength Array”, *Long Wavelength Array Memo*, no. 88, May 2007.

[2] W. C. Erickson, “Tests on Large Blade Dipoles,” *Long Wavelength Array Memo*, no. 36, May 2006.

[3] Retrieved May 31, 2010, from http://lwa.nrl.navy.mil/.

[4] A. Kerkhoff, “The Calculation of Mutual Coupling between Two Antennas and its Application to the Reduction of Mutual Coupling Effects in a Pseudo-Random Phased Array,” *Long Wavelength Array Memo*, no. 103, August 2007.

[5] S. W. Ellingson, T. E. Clarke, A. Cohem, N. E. Kassim, Y. Pihlstrom, L. J Rickard, and G.B. Taylor, “The Long Wavelength Array (invited paper),” *Proc. IEEE*, vol. 97, no. 8, pp. 1421-1430, August 2009.

[6] C. Janes, J. Craig, and L. Rickard, “The Long Wavelength Array System Technical Requirements, Version: Draft #10,” *Long Wavelength Array Memo*, no. 160, Feb. 2009.

[7] B. Hicks et al., “Specmaster: A Simple Spectrum Monitoring Tool,” *Long Wavelength Array Memo*, no. 74, Jan 2007.

[8] T. E. Clarke, “Scientific Requirements for the

Long Wavelength Array," *Long Wavelength Array Memo*, no. 117, Nov. 19, 2007.

[9] W. N. Christiansen and J. A. Högbom, Radiotelescopes, Cambridge University Press, New York, 1969.

[10] L. Kogan and A. Cohen, "A 110 m x 100 m Elliptical Station Design Optimized to Minimize Sidelobes," *Long Wavelength Array Memo*, no. 150, Jan 8, 2009.

[11] P. Henning et.al, "The First Station of the Long Wavelength Array," *Long Wavelength Array Memo*, no. 171, August, 2010.

[12] A. Kerkhof and S. Ellingson, "A Wideband Planar Dipole Antenna for Use in the Long Wavelength Demonstrator Array (LWDA)," *Long Wavelength Array Memo*, no. 18, July 2005.

[13] B. Erickson, H. Schmitt, and E. Polisensky, "Report on Mutual Coupling and Impedance Measurements on Large Blade Dipoles," *Long Wavelength Array Memo*, no. 53, Aug. 2006.

[14] A. Kerkhoff, "Comparison of Dipole Antenna Designs for the LWA," *Long Wavelength Array Memo*, no. 102, Aug 2007.

[15] D. B. Davidson, *Computational Electromagnetics for RF and Microwave Engineering,* Cambridge University Press, New York, 2005.

[16] S. Ellingson, "A Design Study Comparing LWA Station Arrays Consisting of Thin Inverted-V Dipoles," *Long Wavelength Array Memo, no.* 75, January 2008.

Nassissie Fekadu received the B.Sc. degree in Electrical and Computer Engineering from Virginia Tech, Blacksburg, VA in 1999, and the M.S degree in Astronomy from San Diego State University, San Diego, CA in 2005. She is currently working on the Ph.D. degree at Virginia Tech, Falls Church, VA. From 1999-2002, she worked as an RF Engineer at MCI WorldCom Wireless Solutions (Reston, VA), Comsearch (Reston, VA), and Invertix Corporation (Annandale, VA). From 2005-2006 she was a Test and Commissioning Engineer for Andrew Corporation. From 2006-2007 she was a Senior Consultant with Booz-Allen Hamilton, McLean, VA. She has been with Noblis since 2007 as Senior Staff and works as a system engineer to provide technical support to the Federal Aviation Administration (FAA). Her research interests include antennas & propagation, radio astronomy, and wireless communications.

Amir I. Zaghloul is with Virginia Tech and the US Army Research Lab (ARL) on a joint research arrangement. He has been with the Bradley Department of Electrical and Computer Engineering at Virginia Tech since 2001, prior to which he was at COMSAT Laboratories for 24 years performing and directing R&D efforts on satellite communications and antennas. He is a Life Fellow of the IEEE, Fellow of the Applied Computational Electromagnetics Society (ACES), and Associate Fellow of The American Institute of Aeronautics and Astronautics (AIAA). He is a member of Commissions A, B, and Chair of Commission C of the US national Committee (USNC) of the International Union of Radio Science (URSI). He was the general chair of the 2005 "IEEE International Symposium on Antennas and Propagation and USNC/URSI Meeting," held in Washington, D.C., and served as an Ad Com member of the IEEE AP Society in 2006-2009. He also served on the IEEE Publication Services and Products Board and on the Editorial Board of "The Institute." He is a Distinguished Lecturer for the IEEE Sensors Council. He received several research and patent awards, including the Exceptional Patent Award at COMSAT and the 1986 Wheeler Prize Award for Best Application Paper in the IEEE Transactions on Antennas and Propagation.

Dr. Zaghloul received the Ph.D. and M.A.Sc. degrees from the University of Waterloo, Canada in 1973 and 1970, respectively, and the B.Sc. degree (Honors) from Cairo University, Egypt in 1965, all in Electrical Engineering.